Article

The Influence of the Support on the Activity of Mn–Fe Catalysts Used for the Selective Catalytic Reduction of NO$_x$ with Ammonia

Irene López-Hernández, Jesús Mengual and Antonio Eduardo Palomares *

Instituto de Tecnología Química (Universitat Politècnica de València-Consejo Superior de Investigaciones Científicas) Av. De Los Naranjos s/n, 46022 Valencia, Spain; irloher2@posgrado.upv.es (I.L.-H.); jemencu@hma.upv.es (J.M.)
* Correspondence: apalomar@iqn.upv.es

check for updates

Abstract: Mono and bimetallic Mn–Fe catalysts supported on different materials were prepared and their catalytic performance in the NH$_3$–SCR of NO$_x$ was investigated. It was shown that Mn and Fe have a synergic effect that enhances the activity at low temperature. Nevertheless, the activity of the bimetallic catalysts depends very much on the support selected. The influence of the support on the catalyst activity has been studied using materials with different textural and acid–base properties. Microporous (BEA-zeolite), mesoporous (SBA15 and MCM41) and bulk (metallic oxides) materials with different acidity have been used as supports for the Mn–Fe catalysts. It has been shown that the activity depends on the acidity of the support and on the surface area. Acid sites are necessary for ammonia adsorption and high surface area produces a better dispersion of the active sites resulting in improved redox properties. The best results have been obtained with the catalysts supported on alumina and on beta zeolite. The first one is the most active at low temperatures but it presents some reversible deactivation in the presence of water. The Mn–Fe catalyst supported on beta zeolite is the most active at temperatures higher than 350 °C, without any deactivation in the presence of water and with a 100% selectivity towards nitrogen.
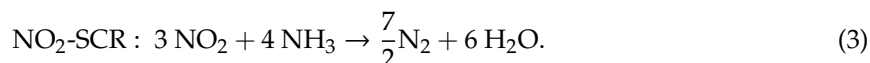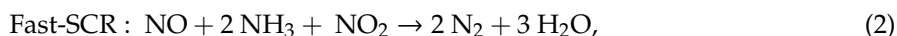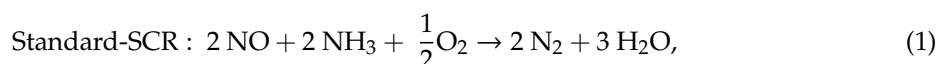
Keywords: NO$_x$; NH$_3$-SCR; Mn; Fe; catalysts; support

1. Introduction

Nitrogen oxides (NO and NO$_2$), are important atmospheric pollutants produced in combustion processes from stationary and mobile sources [1]. They cause severe environmental problems, such as acid rain and principally, photochemical smog, being harmful for ecosystems, humans and animal health [1,2]. These problems, together with the continuous increase of NO$_x$ (nitrogen oxides) emissions and the more stringent regulations result in a necessary control of these emissions both in industry and in transport.

Several techniques have been developed [2] for the control of these pollutants, among them, the selective catalytic reduction of NO$_x$ (NO$_x$–SCR) is probably the most effective one [3]. Different reductants have been used for the NO$_x$ reduction but only ammonia and hydrocarbons are selective enough to be used in a gas stream containing oxygen together with NO$_x$ [4–6]. In the automotive industry, hydrocarbons are initially preferred as reductors as they are present in the exhaust gas, but not many catalysts are active for the reaction and most of them have problems related to the hydrothermal stability of the materials [7]. Ammonia is the other alternative selected by the industry and a high efficiency [8,9] can be obtained when ammonia or its precursor (urea) are used for the NO$_x$–SCR.

The main reactions involved in the selective catalytic reduction of NO_x with ammonia are [10]:

$$\text{Standard-SCR}: \ 2\,NO + 2\,NH_3 + \frac{1}{2}O_2 \rightarrow 2\,N_2 + 3\,H_2O, \tag{1}$$

$$\text{Fast-SCR}: \ NO + 2\,NH_3 + NO_2 \rightarrow 2\,N_2 + 3\,H_2O, \tag{2}$$

$$NO_2\text{-SCR}: \ 3\,NO_2 + 4\,NH_3 \rightarrow \frac{7}{2}N_2 + 6\,H_2O. \tag{3}$$

The catalysts used for these reactions in stationary sources are V_2O_5–MoO_3/TiO_2 and V_2O_5–WO_3/TiO_2 [9,11]. In spite of the high efficiency of these catalysts, their selectivity to N_2 decreases at high temperature and vanadium presents high toxicity preventing its use in cars. Furthermore, some catalysts based in noble metals such as platinum, silver, rhodium and palladium have been proposed [3,12,13] for this reaction. Nevertheless, due the high cost of these materials, the use of transition metals [14] supported on oxides, zeolites or other materials is preferred [15–19]. Cu-zeolites are active catalysts for this reaction but they have problems related with their hydrothermal stability and only small pore zeolites as chabazites are employed for commercial use [20]. For that reason, new alternatives should be explored. The use of other supports, can be an option to modify the performance and stability of the transition metal catalysts. Nevertheless, these supports will modify the dispersion of the active sites and the surface area, and for any specific catalyst, the adequate support must be selected.

Among transition metals, Mn-catalysts have shown excellent low-temperature performance [13,21] due to its redox ability related with the Mn variable valance states [1]. As an example, Fehrmann et al. [22] have shown that monometallic Mn-zeolites are active at 350–500 °C. Furthermore, different bimetallic Mn catalysts have been described as being active and selective for the SCR of NO_x [9,21,23–26], obtaining very good results at low temperature with Fe–Mn catalysts [15,27–33]. Nevertheless, the activity of these catalysts depends on different factors as the metal content, the metal dispersion, the surface area [15,29] and the formation of Fe–Mn mixed phases [34]. These characteristics are determined by the metal-support interaction and different results can be found in the literature for the same active phases, depending on the support used. Some papers claimed that best results are obtained with Mn/Fe catalysts supported on TiO_2 [15,30], whilst others showed the best results with catalysts supported on Al-SBA15 [33] or on mesoporous silica [32]. Nevertheless, the comparison is not easy as they have used different reaction conditions and different metal content. In this work, we have prepared Mn–Fe bimetallic catalysts with 4 wt. % of Mn and 2 wt. % of Fe supported on different materials and their catalytic performance for the NO_x–SCR with NH_3 has been systematically investigated in order to establish the most adequate characteristics of a Mn–Fe catalyst support to be active in this reaction. In this way, we have used supports with different topologies (oxides, microporous and mesoporous materials) and with different acid–base properties. In addition, we have modified the acidity of some supports without changing their nature neither the topology, analysing the influence of these properties in the catalytic activity.

2. Results and Discussion

The different Mn–Fe catalysts used in this work are listed in Table 1. The supports have been selected attending to their different textural and acid–base characteristics. Microporous (beta zeolite), mesoporous (SBA15 and MCM41) and bulk (alumina, zirconia, titania and magnesia) materials have been selected in order to study the influence of the topology of the material on the catalytic activity. The influence of the support acid–base properties on the catalyst activity has been studied using oxides and mesoporous materials with different acidity.

Table 1. Chemical composition and surface area of the catalysts and supports.

Catalyst	wt. % Mn	wt. % Fe	Surface Area (m^2/g)
TiO_2	–	–	90.8
Fe/TiO_2	–	1.79	87.6
Mn/TiO_2	3.75	–	88.1
$Mn–Fe/TiO_2$	3.68	2.21	78.8
ZrO_2	–	–	96.2
$Mn–Fe/ZrO_2$	4.03	2.17	52.8
Al_2O_3	–	–	212.8
$Mn–Fe/Al_2O_3$	3.42	1.95	187.7
MgO	–	–	171.2
Mn–Fe/MgO	4.11	1.83	132.2
MCM-41	–	–	924
Mn–Fe/MCM-41	4.43	2.14	522.9
Al-MCM-41	–	–	1020.2
Mn–Fe/Al-MCM-41	4.80	1.74	989.4
SBA-15	–	–	903.6
Mn–Fe/SBA-15	4.85	2.03	475.9
Al-SBA-15	–	–	967.3
Mn–Fe/Al-SBA-15	3.89	2.08	712.4
BEA	–	–	581.2
Mn–Fe/BEA	4.56	2.03	521.4

The metal content of the mono and bimetallic Mn/Fe catalysts was measured by inductively coupled plasma-optical emission spectrometry (ICP-OES) and the results expressed as wt. % are shown in Table 1. It is observed that for all the samples it is close to the theoretical value (2 wt. % of Fe and 4 wt. % of Mn).

In the same table, the surface area of the catalysts obtained by using the BET (Brunauer–Emmett–Teller) method at relative pressures (p/p^0) ranging from 0.05 to 0.25 is shown. As shown, important differences can be observed depending on the support used. The highest surface areas are obtained with the Al-modified mesoporous Mn–Fe catalysts (Mn–Fe/Al-MCM 41 and Mn–Fe/Al-SBA15) that have surface areas higher than 700 m^2/g. The microporous and the pure silica mesoporous materials (Mn–Fe/SBA15, Mn–Fe/MCM41 and Mn–Fe/BEA) have surface areas close to 500 m^2/g. Al_2O_3 and MgO catalysts have areas higher than 100 m^2/g and the lowest surface areas are obtained for the Mn–Fe catalysts supported on TiO_2 and mainly on ZrO_2.

Initially the activity of the mono and bimetallic catalysts was tested using the TiO_2 (anatase) supported catalysts. As observed in Figure 1, monometallic Fe catalyst only has activity at temperatures above 300 °C, obtaining the maximum conversion at 400–450 °C. On the contrary, the catalyst prepared with Mn is active from 200 °C and reaches the maximum conversion at 300–350 °C. With the bimetallic catalyst, we can observe a positive synergetic effect of both metals, as the results obtained at lower temperatures (100–250 °C) are much better than the results of the addition of the activity of both monometallic catalysts. As observed in Figure 1, the bimetallic catalysts present the highest catalytic activity in the temperature range of 100–375 °C. These results agree with those described by Putluru et al. [15], who showed that the addition of transition metals promotes the activity of Mn/TiO_2 catalysts at low temperatures, probably because they promote the NO oxidation to NO_2 [32]. As this molecule is more reactive than NO [35], the temperature necessary for its reduction decreases and a higher activity at lower temperature is obtained with the bimetallic catalysts.
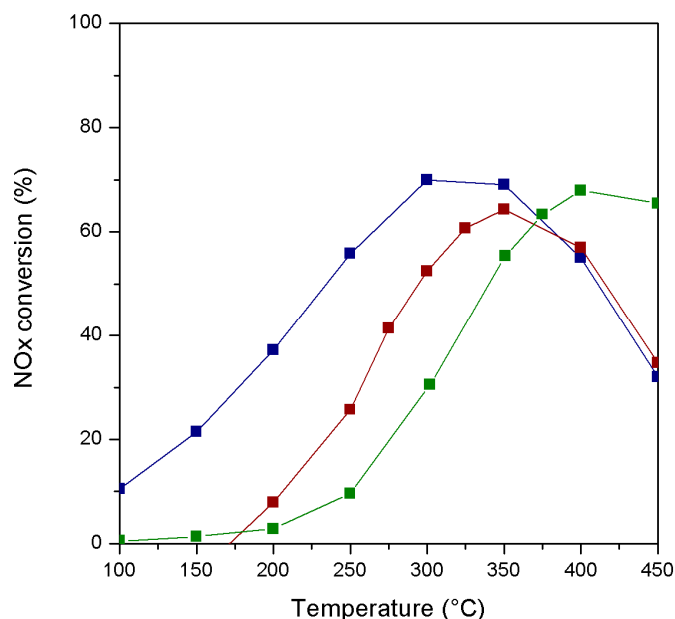
Figure 1. Activity of mono and bimetallic catalysts: (■) Mn–Fe/TiO$_2$, (■) Mn/TiO$_2$ and (■) Fe/TiO$_2$.

The influence of the support on the activity of the Mn/Fe catalysts has been studied with two types of materials: metallic oxides and micro-/mesoporous materials.

Figure 2 shows the catalytic activity of the Mn–Fe catalysts supported on different metallic oxides: TiO$_2$, ZrO$_2$, Al$_2$O$_3$ and MgO. The most significant result is the low activity of the catalyst supported on the most basic support, MgO, in spite of its relatively high surface area. Scaling acidities of metal oxides based on Sanderson electronegativity [36] MgO has a value of 1.266 typical of basic oxides, whilst acidic oxides, as TiO$_2$, have a value of 3.046. Then it can be inferred that acidity is necessary to catalyse this reaction. On the other hand, for the metal oxides with Lewis acid properties (zirconia, alumina and titania) there is a significant relationship between activity at low temperatures and surface area, thus, obtaining the best results with the catalyst that has the highest surface area, i.e., Mn–Fe supported on alumina. These results indicate that not only acidity but also surface area is a key parameter to prepare active Mn–Fe catalysts for this reaction.

The higher specific surface area has been related with an improved dispersion of Fe and Mn on the support resulting in better reduction properties [29]. This was evaluated by thermo-programmed redcution (TPR) experiments with the different materials. The results are shown in Figure 3 corroborating the previous hypothesis. As observed, different peaks related with the reduction of iron and manganese species appear in all the TPR profiles. The assignment of these peaks is not easy as the reduction of manganese oxides takes place in a sequential mode where MnO$_2$ is reduced to Mn$_2$O$_3$, then to Mn$_3$O$_4$ and finally to MnO, overlapping the different peaks [37–39]. According to the literature [40–42] the peak at lowest temperature corresponds to the reduction of MnO$_2$/Mn$_2$O$_3$ to Mn$_3$O$_4$ and the second peak corresponds to the successive reduction of Mn$_3$O$_4$ to MnO. Nevertheless, the manganese oxides formed on the different supports are not pure phases but non-stoichiometric systems [15,29,30] as the overlapping of the different peaks could indicate. Furthermore, some of the reduction peaks of the manganese oxides are coincident with those of iron oxide and can be related with the formation of Mn–Fe mixed oxides [34]. In any case, the comparison of the different TPR profiles, shows that the metal species present in the catalyst with the highest surface area, i.e., that supported on alumina, are reduced at lower temperatures than in the other supports, suggesting better redox properties. This must also be related with the highest activity of this catalyst at low temperatures, indicating that better redox activity results in a better catalytic performance. Then, from the results obtained with the Mn–Fe catalysts supported on different oxides, it can be concluded that for an optimum catalytic activity the selected support must provide acidity, high surface area and redox

properties. This contributes to a better dispersion of the metals on the surface of the catalyst and to the formation of more active sites.
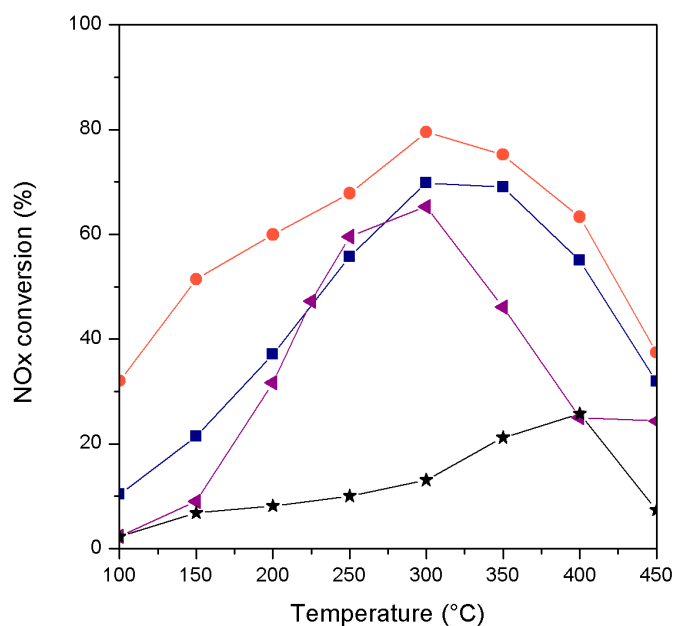

Figure 2. NO_x conversion of bimetallic catalysts supported on different metallic oxides: (■) Mn–Fe/TiO_2, (◀) Mn–Fe/ZrO_2, (●) Mn–Fe/Al_2O_3 and (★) Mn–Fe/MgO.
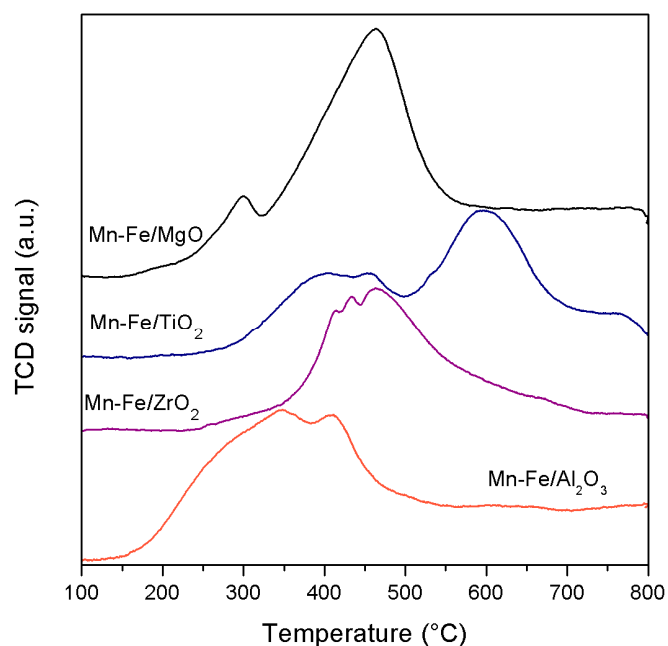

Figure 3. Thermo-programmed reduction (TPR) profile of Mn–Fe catalysts supported on different oxides.

The results obtained with the micro and mesoporous materials are shown in Figure 4. As observed, the catalyst supported on the microporous material (beta zeolite) with a Si/Al ratio of 15 is more active than those supported on pure silica mesoporous materials (MCM41 and SBA15). These results indicate that the microporosity or the presence of aluminium in the BEA zeolite allows a better NH_3-SCR performance.
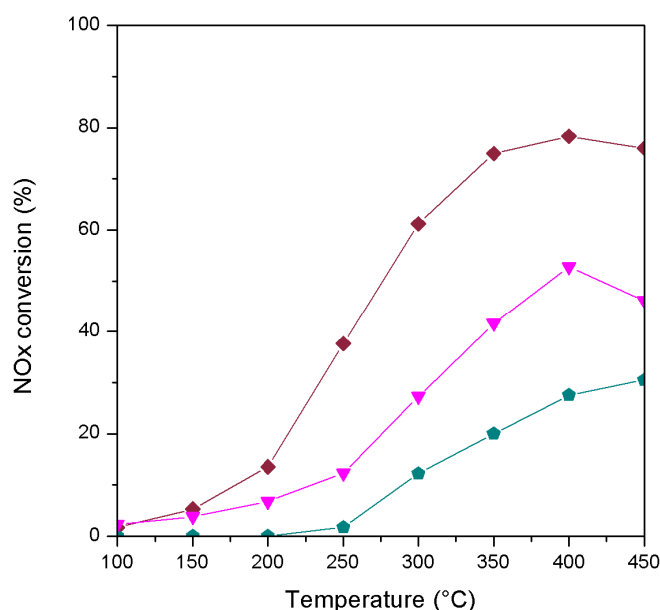
Figure 4. NO$_x$ conversion of Mn–Fe catalysts supported on micro and mesoporous materials: (◆) Mn–Fe/BEA, (⬟) Mn–Fe/MCM-41 and (▼) Mn–Fe/SBA-15.

The role of aluminium was analysed by using some mesoporous materials containing Al and comparing their activity for the NO$_x$–SCR reaction with that of the pure silica materials. As observed in Figure 5 an important increase in the catalyst activity is achieved after incorporation of Al in both MCM-41 and SBA-15. Contrarily to what occurs with the pure silica mesoporous catalysts, in this case the same activity was obtained with both Mn–Fe catalysts containing aluminium. It is described [43–45] that the incorporation of aluminium to a silica mesoporous material produces an enhanced surface acidity, which for the Al-SBA15 results in a Brønsted/Lewis acid sites ratio close to 2–3, mainly medium and weak Brønsted acidity. The larger amount of acidic sites in these materials leads to an improved deNO$_x$ activity, probably related with the necessary primary adsorption of NH$_3$ molecules on the catalyst surface. It is also observed that the Mn–Fe catalysts supported on Al containing mesoporous materials have a higher surface area than those supported on pure silica SBA-15 and MCM-41 and this could contribute to improve the activity of these catalysts.

However, despite the high surface area of these materials, the best results were obtained with the Mn–Fe beta zeolite, that has a 25%–45% lower surface area, microporosity and higher Brønsted/Lewis acid sites ratio (close to 3.8) with stronger Brønsted acidity. Microporosity could favour the dispersion of the active metal sites, even with a lower surface area. The acid properties of the zeolite allows the adsorption of ammonia and the redox properties of the well dispersed Mn–Fe active sites makes easy the NO oxidation to NO$_2$ that will be later reduced to N$_2$ by the adsorbed ammonia. Then the optimum combination of redox and acid properties with microporosity and relatively high surface area results in the highest catalytic activity obtained with the beta zeolite.

The influence of water on the catalytic activity was studied with the more active Mn–Fe catalysts, i.e., those supported on alumina and beta zeolite. The study of the catalyst activity in the presence of water is essential, as this molecule is always present in the combustion processes where the NO$_x$ used to be formed. Figure 6 shows the results obtained when 2.5% of water was added to the reaction. As observed, the addition of water to the reaction does not lead to a decrease in the catalytic activity of the Mn–Fe beta catalyst and only a decrease of activity was observed for the catalysts supported on alumina at low temperatures. On the contrary, such deactivation was suppressed at higher temperatures, even improving the conversion obtained in dry conditions, showing that the inhibiting effect of water is reversible. This indicates that both catalysts present a high stability and that water does not have an important impact on the activity of the catalysts.
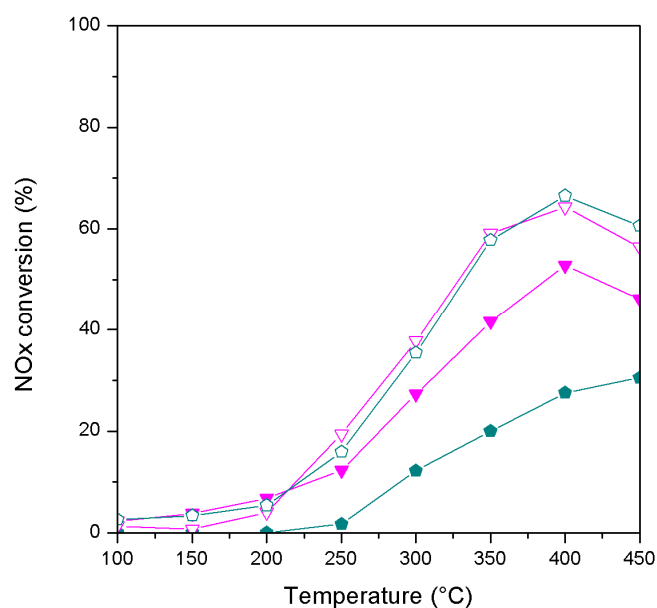
Figure 5. NO$_x$ conversion of Mn–Fe catalysts supported on mesoporous materials with and without aluminium: (⬠) Mn–Fe/MCM-41, (▼) Mn–Fe/SBA-15, (⬡) Mn–Fe/Al-MCM-41 and (▽) Mn–Fe/Al-SBA-15.
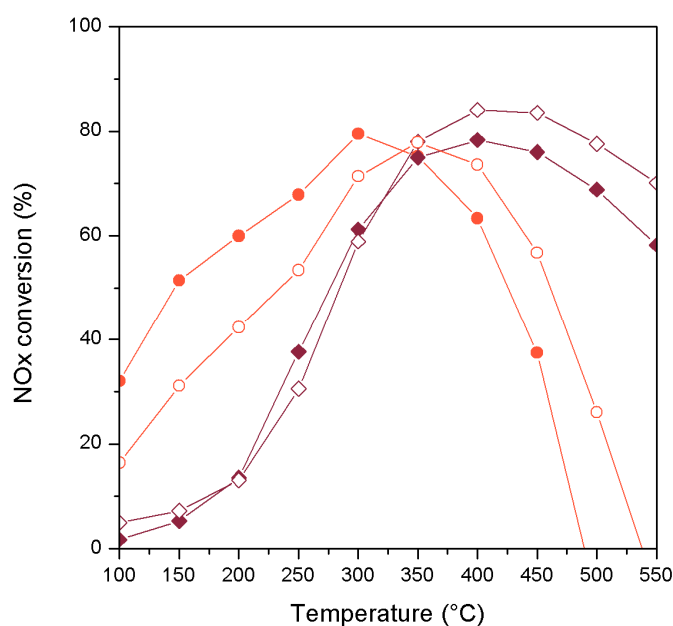

Figure 6. NO$_x$ conversion in presence of water for Mn–Fe catalysts supported on alumina and on beta zeolite: (●) Mn–Fe/Al$_2$O$_3$, (◆) Mn–Fe/BEA, (○) Mn–Fe/Al$_2$O$_3$ (water) and (◇) Mn–Fe/BEA (water).

The selectivity towards N$_2$ was also studied with these catalysts in presence of water. As seen in Figure 7, the catalyst supported on beta zeolite presents a higher selectivity than the Mn–Fe/Al$_2$O$_3$. In fact, almost 100% selectivity towards nitrogen was obtained with the Mn–Fe catalysts supported on BEA zeolites in all range of temperatures, whilst for the catalyst supported on alumina, the selectivity decreases as the temperature increases. This can be related to the partial oxidation of ammonia at these temperatures that is favored in the catalyst supported on alumina. It was reported that isolated iron species promotes N$_2$ selectivity whilst bulk species are unselective [29]. Due to the topology of microporous materials, isolated species are easily formed on the zeolite and this can explain the better

selectivity of the Mn–Fe catalysts supported on beta zeolite if compared with that of the Mn–Fe catalyst supported on alumina.
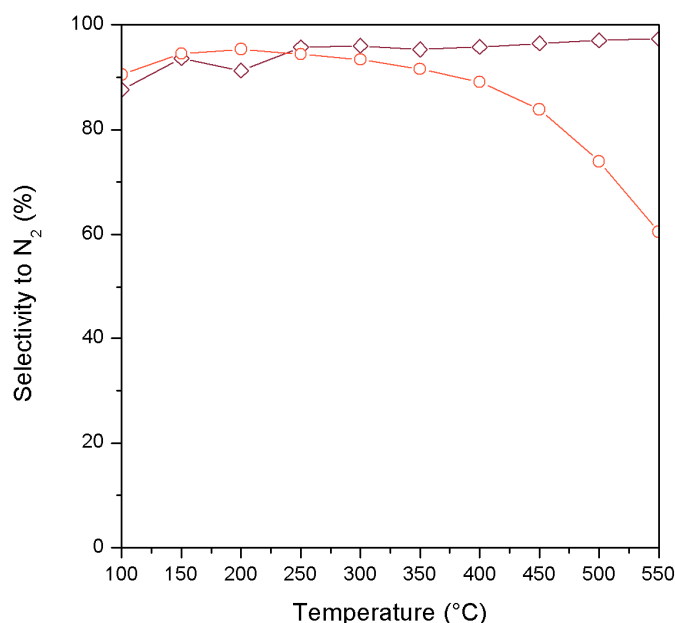

Figure 7. Selectivity to nitrogen in presence of water: (○) Mn–Fe/Al_2O_3 and (◇) Mn–Fe/BEA.

3. Experimental

3.1. Catalyst Preparation

Mn–Fe catalysts were prepared by incipient wetness impregnation using TiO_2, ZrO_2, MgO, BEA zeolite, γ-Al_2O_3, MCM-41 and SBA-15 as supports.

TiO_2 as anatase (CristalACTiV™ DT-51) was purchased from Cristal. ZrO_2 was prepared from hydrolysis of zirconium propoxide [46], BEA zeolite (Si/Al = 18 with 2 wt. % of Al) was obtained from Zeolyst (CP814C) and γ-Al_2O_3 from abcr-GmbH. MCM-41 and SBA-15 were synthetized in our lab following reported methods [47–49]. The mesoporous materials have been prepared as pure silica materials (denoted as MCM-41 and SBA-15) [47], but also with 2 wt. % of aluminium (Al-MCM-41 and Al-SBA-15) [48,49]. Magnesium oxide was prepared in our laboratory from magnesium oxalate by mixing a saturated solution of $Mg(CH_3COO)_2 \cdot 4H_2O$ with an aqueous solution of oxalic acid ($H_2C_2O_4 \cdot 2H_2O$) while stirring at 40 °C. Magnesium oxalate was precipitated, filtered and dried at 100 °C for 24 h. MgO was obtained by calcining the magnesium oxalate at 450 °C in air during 2 h.

Mn–Fe catalysts were prepared by incipient wetness impregnation by adding the desired amount of an aqueous solution of Mn and Fe precursors ($MnCl_2$ and $FeCl_3$) to the precursor in order to obtain a 4 wt. % of Mn and 2 wt. % of Fe. After impregnation, the samples were dried at 100 °C during 24 h, and then calcined at 250 °C for 1 h and at 450 °C for 2 h.

3.2. Catalyst Characterization

The chemical analysis of the catalysts was carried out by ICP-OES in a Varian 715-ES equipment.

H_2-TPR profiles were obtained by a ThermoFinnigan TPDRO1110 analyser using a thermal conductivity detector (TCD). Before H_2-TPR measurements, samples were pre-treated in a quartz U-tube reactor under Ar (30 mL·min^{-1}) at 200 °C and then cooled to 100ºC. The samples were then reduced from 100 to 800 °C under 5% H_2/Ar atmosphere (30 mL·min^{-1}).

BET surface areas were determined from the N_2 adsorption isotherms measured at 77 K using an ASAP-2420 equipment (Micromeritics). Previously to the N_2 adsorption measurements, the samples were heated to 400 °C overnight.

3.3. Catalytic Activity

The activity of the Mn/Fe based catalysts for the SCR reaction was evaluated in a fixed-bed quartz reactor at atmospheric pressure. The reactor was loaded with 400 mg of sieved catalyst (0.4–0.6 mm) using a flow rate of 600 mL·min^{-1} which lead to a gas hour space velocity (GHSV) = 90,000 mL·g^{-1}·h^{-1}. The inlet concentrations were 500 ppm of NO, 500 ppm of NH$_3$, 4% O$_2$ and N$_2$ as balance gas. During the experiments, the temperature was decreased in steps of 50 °C from 550 °C to 100 °C. Before the experiments, samples were kept in an inert atmosphere (nitrogen) during 1 h at 550 °C.

The NO and NO$_x$ concentrations were continuously registered by a Thermo Electron Corporation Model 42 C chemiluminescence gas analyser. The NH$_3$ concentration was monitored in a UV spectroscopy gas analyser from Tethys Instrument, Model EXM400. The N$_2$O concentration was measured with an infrared spectroscopy analyser from Servomex, Model 4900. The NO$_x$ conversion and the selectivity was calculated by Equations (4)–(6):

$$\text{NO}_x \text{ conversion } (\%) = \frac{[\text{NO}_x]_{in} - [\text{NO}_x]_{out}}{[\text{NO}_x]_{in}} \cdot 100, \tag{4}$$

$$\text{N}_2\text{O selectivity } (\%) = \frac{[\text{N}_2\text{O}]_{out}}{[\text{NO}_x]_{in} - [\text{NO}_x]_{out}} \cdot 100, \tag{5}$$

$$\text{N}_2 \text{ selectivity } (\%) = 100 - \text{N}_2\text{O selectivity } (\%), \tag{6}$$

where "in" specify the inlet concentration, and "out" the outlet concentration.

4. Conclusions

From this work, it can be concluded that Mn–Fe catalysts are active for low temperature NO$_x$–SCR with ammonia in the presence of oxygen. Iron and manganese have a synergic effect that improves the catalyst activity at low temperatures. Nevertheless, we have shown that the support has a decisive influence on the activity of the Mn–Fe catalysts for this reaction. The best activity was obtained with catalysts supported on materials with acid sites and high surface area. This results in a better dispersion and in improved redox properties of the metallic active sites. Then, the best results were obtained with the catalysts supported on alumina and on beta zeolite that present these characteristics, whilst the lowest activity was obtained with basic supports or with pure silica mesoporous materials. It is shown that the most active catalysts do not suffer an important deactivation in the presence of water and have a high selectivity towards nitrogen.

References

1. Gao, F.; Tang, X.; Yi, H.; Zhao, S.; Li, C.; Li, J.; Shi, Y.; Meng, X. A Review on Selective Catalytic Reduction of NO$_x$ by NH$_3$ over Mn–Based Catalysts at Low Temperatures: Catalysts, Mechanisms, Kinetics and DFT Calculations. *Catalysts* **2017**, *7*, 199. [CrossRef]
2. Yu, J.J.; Cheng, J.; Ma, C.Y.; Wang, H.L.; Li, L.D.; Hao, Z.P.; Xu, Z.P. NO(x) decomposition, storage and reduction over novel mixed oxide catalysts derived from hydrotalcite-like compounds. *J. Colloid Interface Sci.* **2009**, *333*, 423–430. [CrossRef]
3. Forzatti, P. Present status and perspectives in de-NO$_x$ SCR catalysis. *Appl. Catal. A Gen.* **2001**, *222*, 221–236. [CrossRef]

4. Rutkowska, M.; Díaz, U.; Palomares, A.E.; Chmielarz, L. Cu and Fe modified derivatives of 2D MWW-type zeolites (MCM-22, ITQ-2 and MCM-36) as new catalysts for DeNO x process. *Appl. Catal. B Environ.* **2015**, *168–169*, 531–539. [CrossRef]

5. Palomares, A.; Prato, J.; Imbert, F.; Corma, A. Catalysts based on tin and beta zeolite for the reduction of NOx under lean conditions in the presence of water. *Appl. Catal. B Environ.* **2007**, *75*, 88–94. [CrossRef]

6. Palomares, A.E.; Franch, C.; Corma, A. Determining the characteristics of a Co-zeolite to be active for the selective catalytic reduction of NOx with hydrocarbons. *Catal. Today* **2011**, *176*, 239–241. [CrossRef]

7. Palomares, A.E.; Prato, J.G.; Corma, A. Co-Exchanged IM5, a Stable Zeolite for the Selective Catalytic Reduction of NO in the Presence of Water and SO_2. *Ind. Eng. Chem. Res.* **2003**, *42*, 1538–1542. [CrossRef]

8. Wang, R.; Wu, X.; Zou, C.; Li, X.; Du, Y. NO_x Removal by Selective Catalytic Reduction with Ammonia over a Hydrotalcite-Derived NiFe Mixed Oxide. *Catalysts* **2018**, *8*, 834. [CrossRef]

9. Qi, G.; Yang, R.T. Low-temperature selective catalytic reduction of NO with NH_3 over iron and manganese oxides supported on titania. *Appl. Catal. B Environ.* **2003**, *44*, 217–225. [CrossRef]

10. Forzatti, P.; Nova, I.; Tronconi, E. Enhanced NH3 selective catalytic reduction for NOx abatement. *Angew. Chem. Int. Ed. Engl.* **2009**, *48*, 8366–8368. [CrossRef] [PubMed]

11. Gillot, S.; Tricot, G.; Vezin, H.; Dacquin, J.-P.; Dujardin, C.; Granger, P. Induced effect of tungsten incorporation on the catalytic properties of $CeVO_4$ systems for the selective reduction of NO_x by ammonia. *Appl. Catal. B Environ.* **2018**, *234*, 318–328. [CrossRef]

12. Krishnan, A.T.; Boehman, A.L. Selective catalytic reduction of nitric oxide with ammonia at low temperatures. *Appl. Catal. B Environ.* **1998**, *18*, 189–198. [CrossRef]

13. Li, J.; Chang, H.; Ma, L.; Hao, J.; Yang, R.T. Low-temperature selective catalytic reduction of NO_x with NH_3 over metal oxide and zeolite catalysts—A review. *Catal. Today* **2011**, *175*, 147–156. [CrossRef]

14. Boningari, T.; Smirniotis, P.G. Impact of nitrogen oxides on the environment and human health: Mn-based materials for the NOx abatement. *Curr. Opin. Chem. Eng.* **2016**, *13*, 133–141. [CrossRef]

15. Putluru, S.S.R.; Schill, L.; Jensen, A.D.; Siret, B.; Tabaries, F.; Fehrmann, R. Mn/TiO_2 and $Mn–Fe/TiO_2$ catalysts synthesized by deposition precipitation—Promising for selective catalytic reduction of NO with NH_3 at low temperatures. *Appl. Catal. B Environ.* **2015**, *165*, 628–635. [CrossRef]

16. Chmielarz, L.; Kuśtrowski, P.; Dziembaj, R.; Cool, P.; Vansant, E.F. Catalytic performance of various mesoporous silicas modified with copper or iron oxides introduced by different ways in the selective reduction of NO by ammonia. *Appl. Catal. B Environ.* **2006**, *62*, 369–380. [CrossRef]

17. Chmielarz, L.; Dziembaj, R.; Grzybek, T.; Klinik, J.; Łojewski, T.; Olszewska, D.; Papp, H. Pillared smectite modified with carbon and manganese as catalyst for SCR of NOx with NH_3. Part I. General characterization and catalyst screening. *Catal. Lett.* **2000**, *68*, 95–100. [CrossRef]

18. Gao, Y.; Luan, T.; Zhang, S.; Jiang, W.; Feng, W.; Jiang, H. Comprehensive Comparison between Nanocatalysts of $Mn−Co/TiO_2$ and $Mn−Fe/TiO_2$ for NO Catalytic Conversion: An Insight from Nanostructure, Performance, Kinetics, and Thermodynamics. *Catalysts* **2019**, *9*, 175. [CrossRef]

19. Song, C.; Zhang, L.; Li, Z.; Lu, Y.; Li, K. Co-Exchange of Mn: A Simple Method to Improve Both the Hydrothermal Stability and Activity of Cu–SSZ-13 NH3–SCR Catalysts. *Catalysts* **2019**, *9*, 455. [CrossRef]

20. Paolucci, C.; Di Iorio, J.R.; Ribeiro, F.H.; Gounder, R.; Schneider, W.F. Catalysis Science of NOx Selective Catalytic Reduction With Ammonia Over Cu-SSZ-13 and Cu-SAPO-34. In *Advances in Catalysis*; Elsevier: Amsterdam, The Netherlands, 2016; pp. 1–107. [CrossRef]

21. Wu, Z.; Jiang, B.; Liu, Y. Effect of transition metals addition on the catalyst of manganese/titania for low-temperature selective catalytic reduction of nitric oxide with ammonia. *Appl. Catal. B Environ.* **2008**, *79*, 347–355. [CrossRef]

22. Putluru, S.S.R.; Schill, L.; Jensen, A.D.; Fehrmann, R.S.N. Selective Catalytic Reduction of NOx with NH_3 on Cu-, Fe-, and Mn-Zeolites Prepared by Impregnation: Comparison of Activity and Hydrothermal Stability. *J. Chem.* **2018**, *2018*, 8614747. [CrossRef]

23. Thirupathi, B.; Smirniotis, P.G. Nickel-doped Mn/TiO_2 as an efficient catalyst for the low-temperature SCR of NO with NH_3: Catalytic evaluation and characterizations. *J. Catal.* **2012**, *288*, 74–83. [CrossRef]

24. Peña, D.A.; Uphade, B.S.; Smirniotis, P.G. TiO_2-supported metal oxide catalysts for low-temperature selective catalytic reduction of NO with NH3I. Evaluation and characterization of first row transition metals. *J. Catal.* **2004**, *221*, 421–431. [CrossRef]

25. Qi, G.; Yang, R.T.; Chang, R. MnO$_x$-CeO$_2$ mixed oxides prepared by co-precipitation for selective catalytic reduction of NO with NH$_3$ at low temperatures. *Appl. Catal. B Environ.* **2004**, *51*, 93–106. [CrossRef]

26. Roy, S.B.V.; Hegde, M.S.; Madras, G. Low-Temperature Selective Catalytic Reduction of NO with NH$_3$ over Ti0.9M0.1O2-δ (M) Cr, Mn, Fe, Co, Cu). *J. Phys. Chem. C* **2008**, *112*, 6002–6012. [CrossRef]

27. Shi, J.; Zhang, Z.; Chen, M.; Zhang, Z.; Shangguan, W. Promotion effect of tungsten and iron co-addition on the catalytic performance of MnOx/TiO$_2$ for NH$_3$-SCR of NOx. *Fuel* **2017**, *210*, 783–789. [CrossRef]

28. Husnain, N.; Wang, E.; Li, K.; Anwar, M.T.; Mehmood, A.; Gul, M.; Li, D.; Mao, J. Iron oxide-based catalysts for low-temperature selective catalytic reduction of NO$_x$ with NH$_3$. *Rev. Chem. Eng.* **2019**, *35*, 239–264. [CrossRef]

29. Wang, X.; Wu, S.; Zou, W.; Yu, S.; Gui, K.; Dong, L. Fe-Mn/Al$_2$O$_3$ catalysts for low temperature selective catalytic reduction of NO with NH$_3$. *Chin. J. Catal.* **2016**, *37*, 1314–1323. [CrossRef]

30. Thirupathi, B.; Smirniotis, P.G. Co-doping a metal (Cr, Fe, Co, Ni, Cu, Zn, Ce, and Zr) on Mn/TiO$_2$ catalyst and its effect on the selective reduction of NO with NH$_3$ at low-temperatures. *Appl. Catal. B Environ.* **2011**, *110*, 195–206. [CrossRef]

31. Kim, Y.J.; Kwon, H.J.; Heo, I.; Nam, I.-S.; Cho, B.K.; Choung, J.W.; Cha, M.-S.; Yeo, G.K. Mn–Fe/ZSM5 as a low-temperature SCR catalyst to remove NO$_x$ from diesel engine exhaust. *Appl. Catal. B Environ.* **2012**, *126*, 9–21. [CrossRef]

32. Huang, J.; Tong, Z.; Huang, Y.; Zhang, J. Selective catalytic reduction of NO with NH$_3$ at low temperatures over iron and manganese oxides supported on mesoporous silica. *Appl. Catal. B Environ.* **2008**, *78*, 309–314. [CrossRef]

33. Li, J.; Yang, C.; Zhang, Q.; Li, Z.; Huang, W. Effects of Fe addition on the structure and catalytic performance of mesoporous Mn/Al–SBA-15 catalysts for the reduction of NO with ammonia. *Catal. Commun.* **2015**, *62*, 24–28. [CrossRef]

34. Chen, Z.; Wang, F.; Li, H.; Yang, Q.; Wang, L.; Li, X. Low-Temperature Selective Catalytic Reduction of NO$_x$ with NH$_3$ over Fe-Mn Mixed-Oxide Catalysts Containing Fe$_3$Mn$_3$O$_8$ Phase. *Ind. Eng. Chem. Res.* **2012**, *51*, 202–212. [CrossRef]

35. Palomares, A.E.; Prato, J.G.; Corma, A. A new active zeolite structure for the selective catalytic reduction (SCR) of nitrogen oxides: ITQ7 zeolite the influence of NO$_2$ on this reaction. *Catal. Today* **2002**, *75*, 367–371. [CrossRef]

36. Jeong, N.C.; Lee, J.S.; Tae, E.L.; Lee, Y.J.; Yoon, K.B. Acidity scale for metal oxides and Sanderson's electronegativities of lanthanide elements. *Angew. Chem. Int. Ed. Engl.* **2008**, *47*, 10128–10132. [CrossRef] [PubMed]

37. Sun, M.; Lan, B.; Yu, L.; Ye, F.; Song, W.; He, J.; Diao, G.; Zheng, Y. Manganese oxides with different crystalline structures: Facile hydrothermal synthesis and catalytic activities. *Mater. Lett.* **2012**, *86*, 18–20. [CrossRef]

38. Deng, S.; Zhuang, K.; Xu, B.; Ding, Y.; Yu, L.; Fan, Y. Promotional effect of iron oxide on the catalytic properties of Fe–MnOx/TiO$_2$ (anatase) catalysts for the SCR reaction at low temperatures. *Catal. Sci. Technol.* **2016**, *6*, 1772–1778. [CrossRef]

39. Fang, N.; Guo, J.; Shu, S.; Luo, H.; Chu, Y.; Li, J. Enhancement of low-temperature activity and sulfur resistance of Fe 0.3 Mn 0.5 Zr 0.2 catalyst for NO removal by NH$_3$-SCR. *Chem. Eng. J.* **2017**, *325*, 114–123. [CrossRef]

40. Stobbe, E.R.; de Boer, B.A.; Geus, J.W. The reduction and oxidation behaviour of manganese oxides. *Catal. Today* **1999**, *47*, 161–167. [CrossRef]

41. Fiorenza, R.; Spitaleri, L.; Gulino, A.; Scirè, S. Ru-Pd Bimetallic Catalysts Supported on CeO$_2$-MnO$_x$ Oxides as Efficient Systems for H$_2$ Purification through CO Preferential Oxidation. *Catalysts* **2018**, *8*, 203. [CrossRef]

42. Tu, Y.; Luo, J.; Meng, M.; Wang, G.; He, J. Ultrasonic Ultrasonic-assisted synthesis of highly active catalyst Au/MnO$_x$–CeO$_2$ used for the preferential oxidation of CO in H$_2$-rich stream. *Int. J. Hydrog. Energy* **2009**, *34*, 3743–3754. [CrossRef]

43. Corma, A. From Microporous to Mesoporous Molecular Sieve Materials and Their Use in Catalysis. *Chem. Rev.* **1997**, *97*, 2373–2419. [CrossRef] [PubMed]

44. Gallo, J.M.R.; Bisio, C.; Gatti, G.; Marchese, L.; Pastore, H.O. Physicochemical Characterization and Surface Acid Properties of Mesoporous [Al]-SBA-15 Obtained by Direct Synthesis. *Langmuir* **2010**, *26*, 5791–5800. [CrossRef] [PubMed]

45.　Wu, S.; Han, Y.; Zou, Y.; Song, J.; Zhao, L.; Di, Y.; Liu, S.; Xiao, F. Synthesis of Heteroatom Substituted SBA-15 by the "pH-Adjusting" Method. *Chem. Mater.* **2004**, *16*, 486–492. [CrossRef]

46.　Chuah, G.K.; Liu, S.H.; Jaenicke, S.; Li, J. High surface area zirconia by digestion of zirconium propoxide at different pH. *Micropor. Mesopor. Mat.* **2000**, *39*, 381–392. [CrossRef]

47.　Anne Galarneau, M.N.; Guenneau, F.; di Renzo, F.; Gedeon, A. Understanding the Stability in Water of Mesoporous SBA-15 and MCM-41. *J. Phys. Chem. C* **2007**, *111*, 8268–8277. [CrossRef]

48.　Chen, C.; Li, H.; Davis, M.E. Studies on mesoporous materials I. Synthesis and characterization of MCM-41. *Microp. Mater.* **1993**, *2*, 17–26. [CrossRef]

49.　Li, Y.; Yang, Q.; Yang, J.; Li, C. Synthesis of mesoporous aluminosilicates with low Si/Al ratios using a single-source molecular precursor under acidic conditions. *J. Porous Mater.* **2006**, *13*, 187–193. [CrossRef]